

Submitted to ApJL

Singly-Peaked P-Cygni type Ly α from starburst galaxies

Sang-Hyeon Ahn

*School of Physics, Korea Institute for Advanced Study,
207-43 Cheongnyangri-dong, Dongdaemun-gu, Seoul, 130-722, Korea*

`sha@kias.re.kr`

ABSTRACT

We present results of Monte Carlo calculations for the Ly α line transfer in an expanding dusty supershell, where Ly α source is a well-localized star cluster in a starburst galaxy. The escape of Ly α photons from such system is achieved by a number of back-scattering, and so a series of emission peaks are formed redward of the systemic redshift by back-scattering. However, majority of observed Ly α emission from starbursts show singly-peaked asymmetric profiles. We find in this paper that, in order to form a singly-peaked Ly α emission, dust should be distributed in the ionized bubble, as well as within the supershell of neutral hydrogen. We also find that the overall escape fraction of Ly α photons is determined by the HI column density of the supershell, the expansion velocity of the supershell, and the spatial distribution of dust. However, the kinematic information of the expanding supershell is preserved in the profile of Ly α emission even when the supershell is dusty. Our results are potentially useful to fit the P-Cygni type Ly α line profiles from starburst galaxies, either nearby galaxies or high- z Lyman break galaxies (LBGs).

Subject headings: line: profiles – radiative transfer – method: numerical – galaxies: starburst

1. Introduction

Ly α is the most prominent line feature in the rest-frame ultraviolet (UV) spectra of starburst galaxies, and so Ly α is often used as a redshift indicator. Recently a large number of star-forming galaxies have been spectroscopically observed, either by using the Lyman

break method (Steidel et al. 1996, 1999; Shapley et al. 2003) or by using gravitational lens (Franx et al. 1997; Frye et al. 2002). The detailed review was given by Taniguchi et al. (2003). The rest-frame UV spectra of those galaxies often show unique emission. In these cases, we usually identify this emission as Ly α , and use them as a redshift indicator. Moreover, we propose that this unique feature has more sources of astrophysical information of those star-forming galaxies.

Ly α profiles of starburst galaxies can be classified into three types: P-Cygni type emission, broad absorption, and symmetric emission. The P-Cygni type emission consists of absorption in red part and the asymmetric emission. However, the rest-frame UV continua of high- z galaxies are often too weak to be detected, and so we can only see the asymmetric emission lines. The fraction of symmetric emission is small when compared with the other two types, and thus we will not go into detail of the symmetric type.

Kunth et al. (1998) and Shapley et al. (2003) showed that the kinematics of ambient material is crucial to determine whether emergent Ly α has either broad absorption or P-Cygni type emission. P-Cygni type Ly α emission can be seen only in those galaxies whose interstellar absorption lines are blueshifted with respect to either Ly α emission or stellar atmospheric lines. It seems to be a general consensus that outflowing motion is caused by either galactic superwind or galactic supershell (Lee & Ahn 1998; Heckman et al. 1998; Taniguchi & Shioya 2001; Ahn & Lee 2002; Ahn, Lee, & Lee 2003a,b; Silich et al. 2003; Spinrad 2003). The formation of asymmetric Ly α by outflows was discussed qualitatively by Tenorio-Tagle et al. (1999).

We study in this paper the formation of P-Cygni type Ly α . Ly α radiative transfer is mainly achieved by back-scattering processes in outflowing media. We have studied the role of back-scattering processes in the formation of Ly α line profile (Ahn, Lee, & Lee 2003a,b). For the case of dust-free supershell, we found that a series of peaks appear in the red part of Ly α . In that paper we emphasized that the kinematic motion is imprinted on both the width of each peaks and the velocity difference between peaks. However, majority of the observed Ly α emission lines are dominantly singly peaked. Possibly we can attribute this discrepancy to the previously neglected dust extinction in the radiative transfer. We study in this paper the Ly α line formation mechanism by interplay among the Ly α resonance scattering in optically thick supershell of neutral hydrogen, the spatial extension of dust in the HII bubble, and the kinematics of the supershell with respect to Ly α sources at the center of the supershell.

2. Model

Galactic supershells are very well-known structures in the nearby starburst galaxies (Marlowe et al. 1995; Martin 1998; Korthes & Kerton 2002). Their origin is known to be multiple explosions of the supernovae in active star-forming regions. In this paper we adopt a model galaxy of high- z starburst galaxies in which Ly α sources are presumed to be located at a restricted part of the galaxy and surrounded by a dusty galactic supershell. The supershell is assumed to be made of uniform medium of neutral hydrogen and expanding in a bulk manner. We assume that the interior of the supershell is fully ionized, which is vacuum in the sense of Ly α scattering. The model in this study is very simple, and it has several model parameters. However, the main purpose of this paper is to emphasize the role of spatial distribution of dust in destroying the secondary and higher peaks. We will itemize and clarify the assumptions in this study as follows.

1. The starbursting region is assumed to be localized in a region of the model galaxy. This assumption is based on the fact that almost all the observed Ly α emission lines are asymmetric. If the galaxy were rotating and its star-forming regions are scattered along spiral arms, we might see symmetric Ly α emission lines. Hence we can consider that the star-forming regions are localized in a rather narrow region in the galaxies. The HST images of about half of the LBGs show the amorphous shape of those high- z galaxies, while the other half show the nuclear starburst (Calzetti & Giavalisco 2001). Here we assume that even in the amorphous galaxies, only the brightest star-forming region is a dominant source of Ly α photons.
2. The ionized inner part of the supershell can also be a source of Ly α photons. However, the fraction of photons, generated in the ionized part of the supershell, is smaller than that of the stellar Ly α photons (Tenorio-Tagle et al. 1999). Moreover, there is no kinematic difference between the photons back-scattered by the neutral supershell and the photons emitted by ionized supershell. Hence we will neglect photons emitted from the ionized inner part of the supershell.
3. We adopt a typical width of input Ly α profile $\sigma_{\text{Ly}\alpha} = 50 \text{ km s}^{-1}$ in this paper. Legrand (1997) observed H α emission of a nearby HII galaxy Haro 2. The H α line width is $\sigma_{\text{H}\alpha} = 50 \text{ km s}^{-1}$ which is equivalent to $\sigma_{\text{Ly}\alpha} = 50 \text{ km s}^{-1}$. The input line width of Ly α affects the width of emergent emission peaks. However, it ranges between 50 and 115 km s $^{-1}$ (Pettini et al. 2001), which justifies our choice.
4. The continuum is neglected in this paper. According to Shapley et al. (2003), the Ly α profiles for 38% of their sample of LBGs consist of a combination of both emission

and absorption. The equivalent width (EW) of broad absorption is $10 - 20\text{\AA}$, which will be dumped in the red wing of the primary peak. However, those photons must be partially destroyed by dust extinction. Moreover, dust-free galaxies would have Ly α equivalent widths of $50 - 200\text{\AA}$ (Charlot & Fall 1993), which is much larger than the absorption EW of the continuum. Hence we assume that the continuum will give a minor contribution.

5. We also assume that the galactic supershell fully covers the starburst region, and that $R_{min} = 0.9R_{max}$. Here R_{max} is the outer radius of the supershell and R_{min} is the inner radius of the supershell.
6. We also assume that the HI column density outside the supershell is negligible, because the supershell is assumed to be of galactic scale. We adopt the column density of neutral hydrogen $N_{\text{HI}} = 10^{19} - 10^{20}\text{cm}^{-2}$ in accordance with Voigt fittings done by Kunth et al. (1998). This column density corresponds to the line-center optical depth by $\tau_0 \equiv 2.27 (b/80 \text{ km s}^{-1})^{-1} [N_{\text{HI}}/10^{14}\text{cm}^{-2}]$. Here b is the Doppler parameter corresponding to turbulence, which is typically 80 km s^{-1} for nearby HII galaxies (Kunth et al. 1998). This gives us the Voigt parameter $a = 7.60 \times 10^{-5} (80 \text{ km s}^{-1}/b)$.
7. We also assumed for simplicity that the neutral hydrogen in the supershell is uniformly distributed. In fact, the supershell can either be patchy or have density gradient, which is also important for escape of Lyman limit photons. The geometry of the supershell is assumed to be spherical for simplicity. The supershell evolves more rapidly toward the steepest density gradient (Silich & Tenorio-Tagle 1998), but it evolves to be of galactic scale. Thus we can assume that the supershell is spherical. However, more work for complicated geometry can be expected in future work.
8. We adopt the typical expansion velocity of the supershell $V_{exp} = 200 \text{ km s}^{-1}$. According to Kunth et al. (1998), the neutral gas in nearby starburst galaxies along the line of sight is being pushed by an expanding envelope around the HII region, outflowing at velocities close to 200 km s^{-1} . Moreover, in the composite spectrum of high- z galaxies, Shapley et al. (2003) measured an average blueshift for the strong low-ionization interstellar features of $\Delta v = -150 \pm 60 \text{ km s}^{-1}$ with respect to the stellar systemic redshift. Thus we adopt $V_{exp} = 200 \text{ km s}^{-1}$ as a typical value.
9. The bulk expansion is assumed, although there can be radial velocity gradient in the supershell. The real supershell must be complex, but we restrict the current scope of study within cases of bulk expansion. Here the bulk expansion implies that dust and gas are also strongly coupled.

10. We assume that dust is distributed uniformly in the ionized bubble, as well as within the supershell. When we let R_d be the inner radius of the dust shell, R_d can be less than R_{min} . The outer radius of dust shell is assumed to be equal to R_{max} . Although the dust size distribution and the number density are surely altered by the shock waves, we assume in this paper that they are same both in the ionized bubble and within the supershell.
11. We defined a radial dust opacity through the dust shell τ_d , in order to reconcile with the usual way of estimating dust opacity by analyzing the extinction of the UV continuum from central stars in the central region of HII region. Another important physical parameter related with dust abundance is dust-to-gas ratio. In particular, we define the dust-to-HI ratio in the neutral supershell by $\mathbf{D} = \tau_d/\{N_{\text{HI}}\sigma_d(1 - A)\}\{(R_{max} - R_{min})/(R_{max} - R_d)\}m_d/m_{\text{HI}}$. Here the typical mass of grains is defined by $m_d = 4\pi/3a_d^3\rho_d$, σ_d is the absorption cross-section of dust grains, A is albedo, m_{HI} is the mass of hydrogen atom, and a_d is the radius of dust grains effective at 1216Å. We adopt the mass density of dust grains $\rho_d = 1\text{ g cm}^{-3}$ and the size of dust grain $a_d = 1.9 \times 10^{-6}\text{ cm}$. We adopt the typical albedo $A = 0.5$ in accordance with Draine & Lee (1984).

We use the Monte Carlo method whose detailed description was presented in our previous papers (Ahn, Lee, & Lee 2000, 2001, 2002, 2003a). In the Monte Carlo code, we calculate the integrated path lengths of a Ly α photon before its escape only if the photon is passing through the dust shell. Thus the integrated dust opacity experienced by the photon is given by $\tau_d^e = \tau_d/\tau_0 \sum_i S_i$. Here S_i is a path length in units of τ_0 along which a Ly α photon propagates between the $(i - 1)$ -th scattering and the i -th scattering within the dust shell in $R_d < r < R_{max}$. A more detailed description of the Monte Carlo code for dust-free supershell was given in Ahn, Lee, & Lee (2003b).

3. Results

We present the emergent profiles which are calculated using the Monte Carlo method in Figures 1 and 2. We can see that there are two peaks for each case, which is similar to our previous study (Ahn, Lee, & Lee 2003a,b). We call the peaks at $V \simeq V_{exp}$ the primary peaks, and the peaks at $V \approx 3V_{exp}$ the secondary peaks. Figure 1 show the emergent profiles for $N_{\text{HI}} = 10^{19}\text{ cm}^{-2}$ and $N_{\text{HI}} = 10^{20}\text{ cm}^{-2}$. When we compare the left panels with $R_d = 0.4R_{max}$ to the right panels with $R_d = 0.9R_{max}$, we can see that the secondary peaks are destroyed efficiently if the dust shell extends into the ionized bubble (i.e. cases with $R_d = 0.4R_{max}$).

This fact means that the emergent Ly α photons, forming the peaks, have experienced

almost the same amount of dust extinction, if dust is distributed only within the supershell. This can be explained as follows. Every back-scattering causes redshift of Ly α photons. Since the supershell is optically very thick, Ly α photons are back-scattered at the shallow inner part of the supershell. Hence, the dust opacity contributed by path length within the supershell is relatively small, and the contribution during the final escape dominates the total dust opacity. Hence, the total dust opacity for most of Ly α photons escaped after back-scattering becomes similar, which results in the inefficient decrease of secondary peaks.

The situation becomes different when the dust shell extends into the ionized bubble, $R_d < R_{min}$. While they are scattered back and forth in the bubble by back-scattering, the Ly α photons are redshifted and eventually escape to form the secondary and the tertiary peaks. Thus, back-scattered Ly α photons have large path length within the dust shell in the ionized bubble. The dust opacity contributed by the dust shell within the ionized bubble is roughly proportional to the number of back-scattering. Hence the secondary and the tertiary peaks are more rapidly decreased than the primary peak.

The survival fraction of Ly α photons is mostly affected by the dust opacity within the supershell, which is determined by two factors; one is the dust opacity within the supershell, and the other is the integrated path length within the supershell. According to theoretical researches (Adams 1972; Harrington 1973; Neufeld 1990; Ahn, Lee, & Lee 2002), we usually call the medium extremely thick when $a\tau_0 \geq 10^3$. In this case, a Ly α photon experiences a large number of resonance core scattering, during which it happens to scatter with a hydrogen atom fastly moving at the tails of the Boltzmann velocity distribution. Then, the photon becomes a wing photon, for which the medium is transparent. The wing photon restores gradually to the core photon while it experiences a series of wing scattering, during which the photon wanders around the medium. This wandering can be regarded as a spatial diffusion, and can be described by random walk process. The photon has now core frequency again, and it repeats such processes. We call this one cycle an excursion. During such an excursion, Ly α can escape the medium. As a corollary, Ly α photons suffer a larger amount of dust extinction either when the integrated path length of those photons within the supershell is increased or when the dust opacity within the supershell is very high.

Firstly, the dust opacity within the supershell is $\tau_d(R_{max} - R_{min})/(R_{max} - R_d)$. Thus, although the HI column densities are same, the dust opacity within the supershell increases as R_d approaches to R_{min} . As a result, in Figure 3, the survival fraction curves for $R_d = 0.9R_{max}$ are steeper than those for $R_d = 0.4R_{max}$ for cases with the same N_{HI} and b .

Secondly, as $a\tau_0$ increases, both the number of wing scattering per excursions and the number of excursions within the supershell increases. Hence, the path length within the supershell is an increasing function of $a\tau_0$. In Figure 3, for cases with the same Doppler

parameter $b = 80 \text{ km s}^{-1}$, we can see that the curve with $N_{\text{HI}} = 10^{20} \text{ cm}^{-1}$ is decreased much faster than that with $N_{\text{HI}} = 10^{19} \text{ cm}^{-1}$.

Thirdly, we know in Section 2 that that $a \propto b^{-1}$ and $\tau_0 \propto b^{-1}$. Thus, $a\tau_0 \propto b^{-2}$. Since the number of excursion within the supershell is proportional to $a\tau_0$. We can expect that the destruction of the secondary and higher peaks is enhanced for small b . We show in Figure 2 the changes of profiles for different Doppler widths, when both the column density of neutral hydrogen N_{HI} and the dust configuration (or R_d and τ_d) are same. The secondary peak is decreased more rapidly as b is decreased. In addition, the width of the primary peaks decreases for small b . The red part of the primary peak is formed of the photons which are scattered backward. Those photons experiences dust extinction both within the supershell by resonance scattering and in the dust shell. Thus they can be easily destroyed by dust during those scattering processes, and so the primary peak becomes narrow. We show in Figure 3 the variation of survival fraction of Ly α photons for the cases of different Doppler parameters, while N_{HI} , τ_d , and R_d are same. When we compare the solid line with solid dots with the dotted line with solid dots, we can see that the curve for cases with small b decreases rapidly.

On the other hand, we can see in Figures 1 and 2 that both the widths of peaks and the velocity difference between peaks are largely insensitive to dust opacity. We showed that the kinematics of outflowing material is imprinted on both the velocity width of the peaks and the velocity differences between peaks (Ahn, Lee, & Lee 2003a,b). Therefore, those characteristics can be used potentially to estimate the expansion velocity of the supershell even in dusty interstellar media.

4. Summary

In this paper we emphasize that the spatial distribution of dust grains in the supershell is as important in forming the P-Cygni type Ly α emission profiles as the kinematics of the supershell. The escape probability of Ly α photons is greatly enhanced when the supershell is expanding with respect to the central Ly α sources. That is, the Ly α resonance scattering is off-centered and the escape probability of Ly α photons is enhanced. As the number of back-scattering increases, Ly α photons are redshifted more and more, which enhances the escape probability. Ly α photons are scattered backward by high HI column density of expanding supershell. Therefore, in the cases of dust-free supershell, these back-scattering processes result in a series of peaks in the redward of Ly α . However, majority of observed Ly α emission show no such peaks. In this paper, we have found that the single peak can be formed, only when dust extends in the ionized bubble, as well as within the supershell. In this case,

the integrated path length in dust shell increases as Ly α photons scatter back and forth by the shallow part of the inner wall of the supershell. Thus, the integrated dust opacities increases as the inner radius of the dust shell decreases, which is main discovery of this study. Moreover, when Ly α photons suffer a large number of resonance core scattering and wing scattering within the supershell, their path lengths become very large. Thus, the dust opacity within the supershell is also one of decisive factor that determines the overall escapability of Ly α photons. Furthermore, both the optical depth and the Doppler parameter of the supershell are another crucial factor to determine the survival fraction of Ly α photons. We have found that the kinematic information of outflowing media surrounding Ly α sources is imprinted on the Ly α profiles, and it is conserved even when the medium is dusty. However, our model is very simplified one, whose limitation is described in Section 2 in detail. More work is needed in the future.

REFERENCES

Adams, T. 1972, ApJ, 174, 439

Ahn, S. -H., Lee, H. -W., & Lee, H. M. 2000, J. of Korean Astron. Soc., 33, 29

Ahn, S. -H., Lee, H. -W., & Lee, H. M. 2001, ApJ, 554, 1

Ahn, S. -H., Lee, H. -W., & Lee, H. M. 2002, ApJ, 567, 922

Ahn, S. -H., & Lee, H. -W. 2002, J. of Korean Astron. Soc. , 35, 175

Ahn, S. -H., Lee, H. -W., & Lee, H. M. 2003a, in ASP Conf. Ser. 289, Proceedings of the IAU 8th Asian-Pacific Regional Meeting, Volume II, ed. S. Ikeuchi, J. Hearnshaw, and T. Hanawa, (Tokyo: the Astronomical Society of Japan), 243

Ahn, S. -H., Lee, H. -W., & Lee, H. M. 2003b, MNRAS, 340, 863

Calzetti, D., & Giavalisco, M. 2001, Astrophysics and Space Science Supplement, 277, 609

Charlot, S., & Fall, S. M. 1993, ApJ, 415, 580

Draine, B. T., & Lee, H. M. 1984, ApJ, 285, 89

Franx, M., Illingworth, G. D., Kelson, D. D., van Dokkum, P. G., & Tran, K. 1997, ApJ, 486, 75

Frye, B., Broadhurst, T., & Benítez N. 2002, ApJ, 568, 558

Harrington, J. P. 1973, MNRAS, 162, 43

Heckman, T. M., Robert, C., Leitherer, C., Garnett, D., & van der Rydt, F. 1998, ApJ, 503, 646

Kothes, C., & Kerton, C. R. 2002, A&A, 390, 337

Kunth, D., Mas-Hesse, J. M., Terlevich, E., Terlevich, R., Lequeux, J., & Fall, S. M. 1998, A&A, 334, 11

Legrand, F., Kunth, D., Mas-Hesse, J. M., Lequeux, J. 1997, A&A, 326, 929

Lee, H. -W., & Ahn, S. -H. 1998, ApJ, 504, L61

Marlowe, A. T., Heckman, T. M., Wyse, R. F. G., & Schommer, R. 1995, ApJ, 438, 563

Martin, C. 1998, ApJ, 506, 222

Neufeld, D. A. 1990, ApJ, 350, 216

Pettini, M., Shapley, A. E., Steidel, C. C., Cuby, J., Dickinson, M., Moorwood, A. F. M., Adelberger, K. L., Giavalisco, M. 2001, ApJ, 554, 981

Shapley, A. E., Steidel C. C., Pettini, M., & Adelberger, K. L. 2003, ApJ, 588, 65

Silich, S. A., & Tenorio-Tagle G. 1998, MNRAS, 299, 249

Silich, S. A., Tenorio-Tagle G., & Muñoz-Tuñón, C. 2003, ApJ, 590, 791

Spinrad, H. 2003, Astrophysics Update, in press, ed. J. Mason, Springer Praxis Books in Astrophysics and Astronomy, Praxis 2004 (astro-ph/0308411)

Steidel, C. C., Giavalisco, M., Pettini, M., Dickinson, M., & Adelberger, K. L. 1996, ApJ, 462, 17

Steidel, C. C., Adelberger, K. L., Giavalisco, M., Dickinson, M., & Pettini, M. 1999, ApJ, 519, 1

Taniguchi, Y., & Shioya, Y. 2001, ApJ, 547, 146

Taniguchi, Y., Shioya, Y., Ajiki, M., Fujita, S., Nagao, T., & Murayama, T. 2003, J. of Korean Astron. Soc., in press (astro-ph/0306409)

Tenorio-Tagle, G., Silich, S. A., Kunth, D., Terlevich, E., & Terlevich, R. 1999, MNRAS, 309, 332

Whittet, D. C. B. 1990, Dust in the Galactic Environment, (London: the Institute of Physics), 73

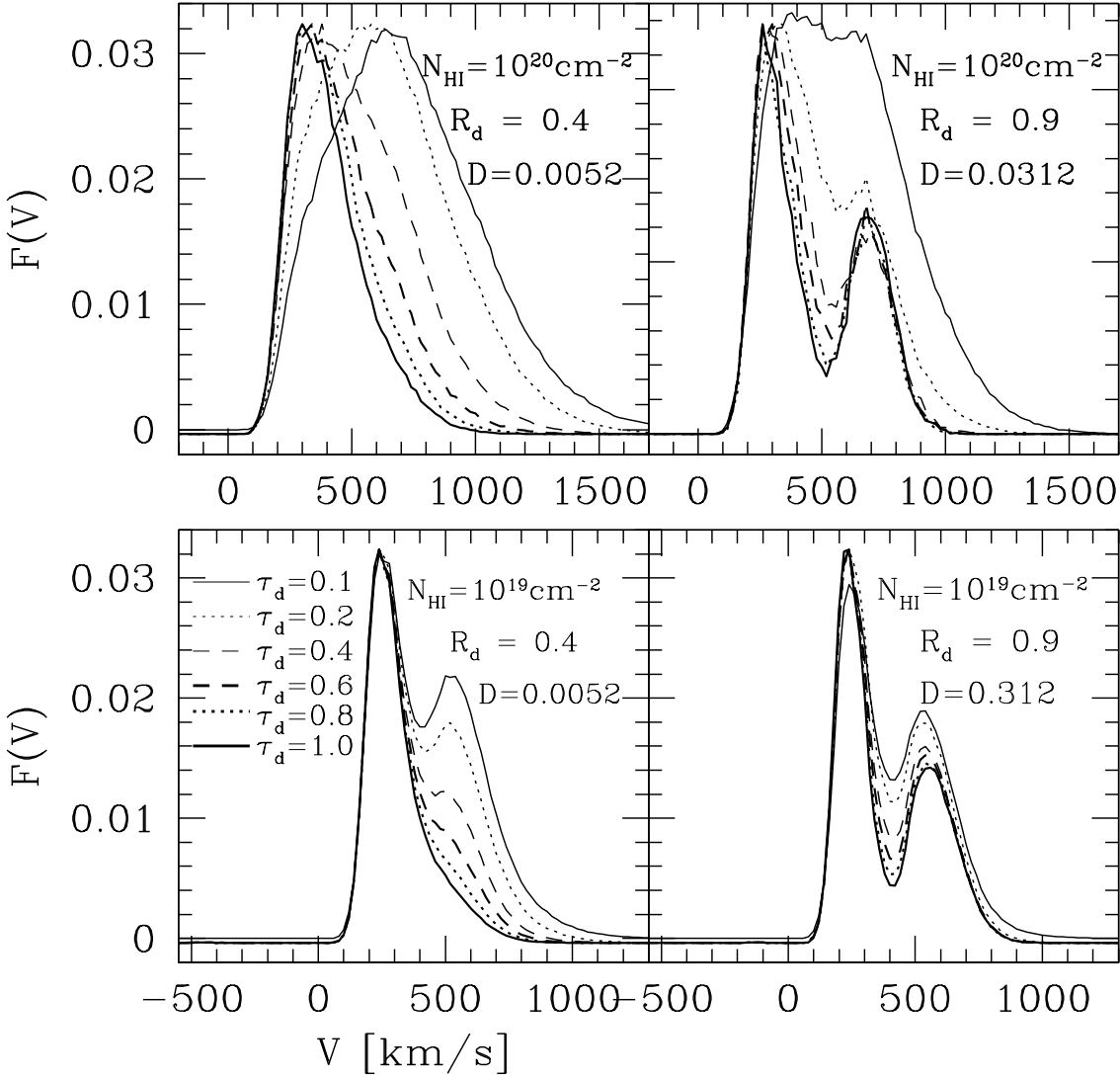


Fig. 1.— Profiles of emergent Ly α emission. The upper panel is for cases with $N_{\text{HI}} = 10^{20} \text{ cm}^{-2}$, and the lower panel is for cases with $N_{\text{HI}} = 10^{19} \text{ cm}^{-2}$. The inner radii of cases in the left panels are $0.4R_{\text{max}}$, and those of left panels are $0.9R_{\text{max}}$. The expansion velocity of the supershell $V_{\text{exp}} = 200 \text{ km s}^{-1}$, and the Doppler parameter $b = 80 \text{ km s}^{-1}$ in common. In order to show the relative flux ratio between the primary and the secondary peaks, all the profiles are normalized with respect to the primary peak. The vertical coordinate means flux, and the survival fraction of Ly α photons is shown in Figure 3. The dust-to-gas ratios in the supershell for $\tau_d = 1$ are given in each box. Note that the dust-to-(HI+He) ratios of Our Galaxy and the Large Magellanic Cloud are 0.007 and 0.002, respectively (Whittet 1992).

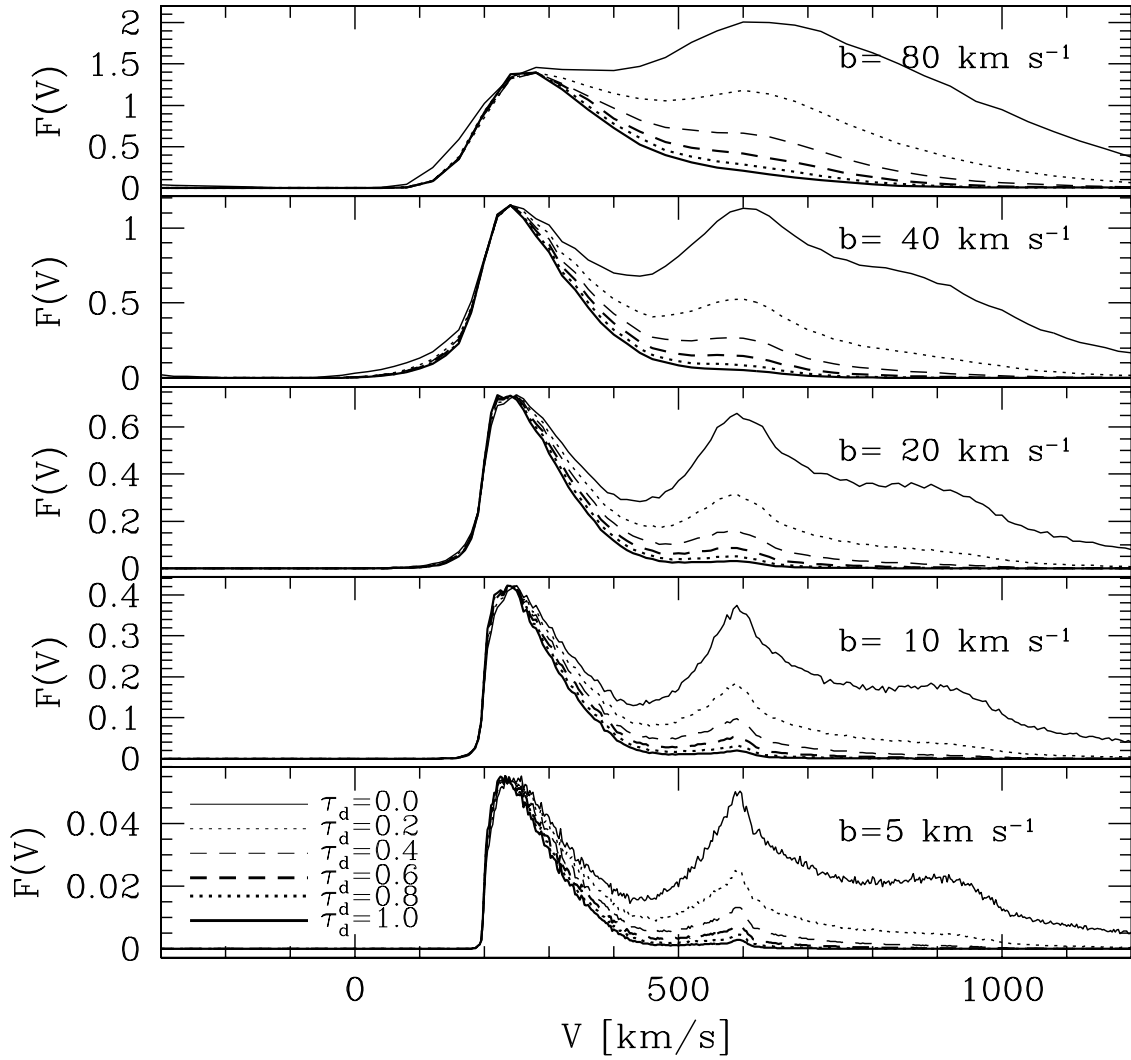


Fig. 2.— Profiles of emergent Ly α emission for cases with different Doppler widths and same other parameters ($N_{\text{HI}} = 10^{19} \text{ cm}^{-2}$, $V_{\text{exp}} = 200 \text{ km s}^{-1}$, $R_d = 0.4R_{\text{max}}$). All the profiles are normalized with respect to the primary peak. The relative strength is represented by dotted lines of survival fraction curves in Figure 3. Note that the secondary peaks decreases more sensitively as b decreases.

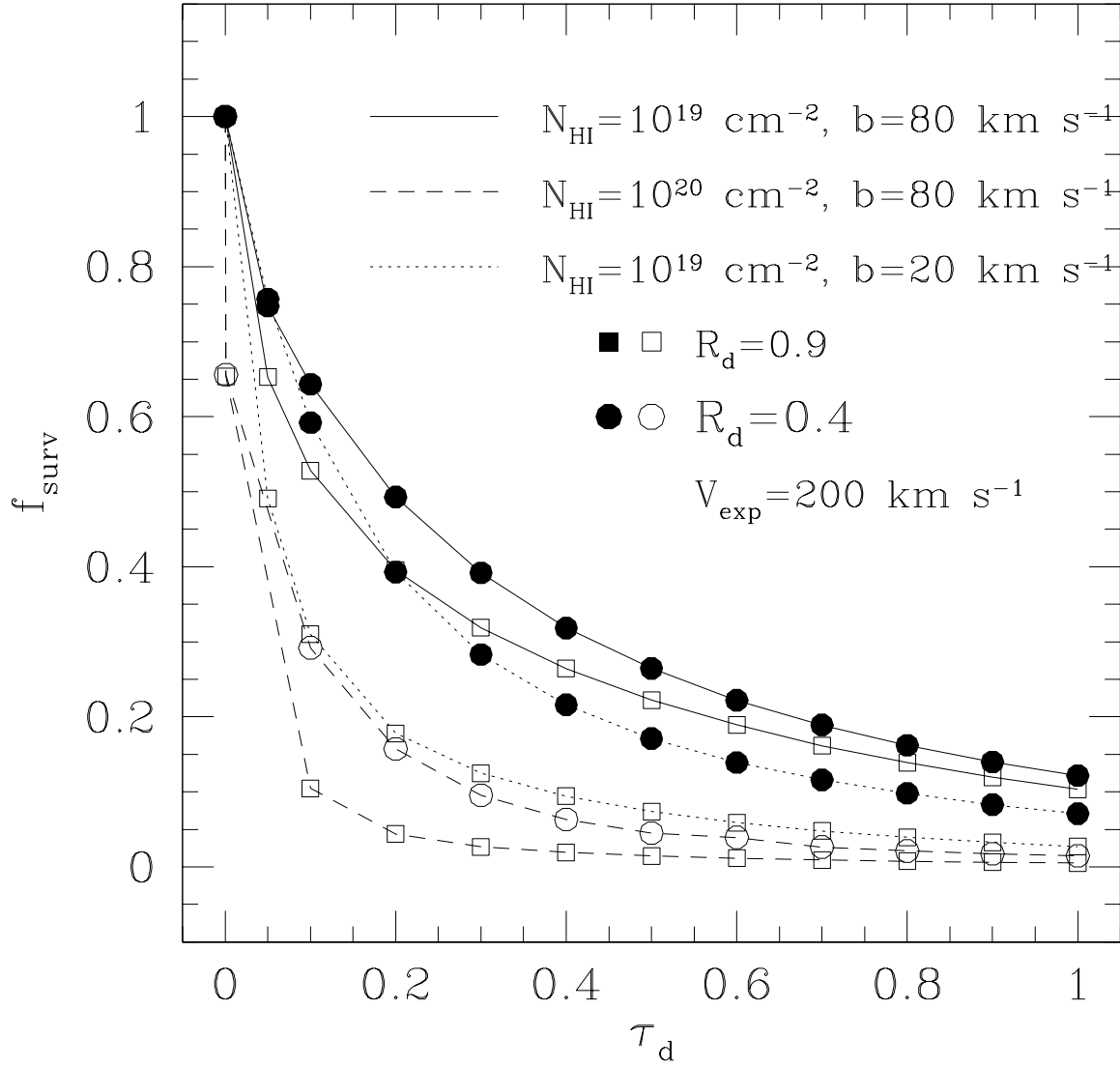


Fig. 3.— Survival fraction of Ly α photons with dust opacities. The model parameters of the supershell is given in the figure. We can see that more Ly α photons are destroyed as R_d increases to reach R_{\min} . However, we see in Figures 1 and 2 that the secondary peak is more rapidly decreased as R_d decreases.